# REMOVAL OF THE EFFECT OF COMPTON SCATTERING IN 3-D WHOLE BODY POSITRON EMISSION TOMOGRAPHY BY MONTE CARLO

C.S. Levin, Y-C Tai, E.J. Hoffman, M. Dahlbom, T.H. Farquhar
UCLA School of Medicine Division of Nuclear Medicine and Biophysics
Los Angeles, CA 90095

*Abstract*

A Monte Carlo technique has been developed to simulate and correct for the effect of Compton scatter in 3-D acquired PET whole body imaging. The method utilizes the attenuation corrected and normalized, 3-D reconstructed image volume as the source intensity distribution for a photon-tracking Monte Carlo simulation. It is assumed that the number of events in each pixel of the image represents the isotope concentration at that location in the body. The history of each annihilation photon's interactions in the scattering media is followed. The edges and average attenuation coefficients of the various scattering media are determined using a segmented image volume derived from a short transmission scan. The sinograms for the scattered and unscattered photon pairs are generated in a simulated 3-D PET acquisition. The calculated scatter contribution is used to correct the original data set. The method is general and can be applied to any scanner configuration or geometry. In its current form the simulation requires 20 hours on a Sparc10 when every pixel in a 89-plane, 128x128 pixel, 3-D acquired (CTI 961, two bed positions) image volume is sampled, and roughly 1 hour when 16 pixels (4x4) are grouped as a single pixel. In this report we present results of the scatter correction method using a 3-D acquired human study of the thorax as input.

## I. INTRODUCTION

In order for PET to realize its full potential in terms of spatial resolution and signal to noise ratio, many systems are now designed with retractable inter-plane septa, allowing all possible lines of response to be acquired. The increased sensitivity (ca. 5-7 fold) of three-dimensional (3-D) PET acquisition is especially useful when long scan times are required, as with multiple bed position whole body studies. Unfortunately, this 3-D mode of acquisition results in a large (ca. 3-8 fold) increase in scatter fraction relative to conventional two-dimensional data collections with septa. This increase in scatter compromises accuracy in quantitation and degrades image contrast. The development of an accurate and efficient scatter correction is desirable for the removal of image distortions which might lead to diagnostic errors, and essential before quantitative measurements can be made with 3-D PET.

The motivation for developing a Monte Carlo correction for Compton scatter in 3-D whole body PET is twofold: 1) For 2-D PET, one had a situation in which scatter was a 10-20% effect added to a technique that realistically expects no better than 10% accuracy. In that case, a 30% error in the scatter estimate would cause only a 3 to 6% error in the result. For 3-D whole body PET, the scatter component dominates the trues (see Section III, Figure 1), and errors in the scatter estimate become large compared to other systematic errors; a higher degree of accuracy in the scatter correction is, thus, required. 2) For 3-D whole body PET, an accurate and efficient scatter correction is desirable to avoid diagnostic errors in whole-body surveys for tumor metastases. The generally poor statistics and large imaging area required puts strict limitations on the types of scatter corrections that are appropriate. Because the data sets are large and of low resolution, the scatter correction method must be fast but not necessarily of high resolution. We thus emphasize the use of coarse sampling of the Monte Carlo input.

We have previously demonstrated [1] the Monte Carlo scatter correction technique applied to 3-D PET brain imaging. In that paper other scatter correction schemes for 3-D PET were described. Most of these other methods use approximations or models of scatter that are presumed to be valid without regard to the source distribution and attenuating media. Scatter distributions for realistic sources and scattering media do have a significant dependence on the source distribution and object composition and shape. Most generalizations or simplifying assumptions should not be expected to hold for all situations and will compromise accuracy. In addition, methods that require supplementary measurements introduce additional noise and may require longer patient scanning time and/or larger data sets.

Our Monte Carlo scatter correction method is isotope distribution dependent and models the statistical and physical process of photon emission. The scatter distribution is simulated for complex activity and density distributions using the physics of photon interactions. No assumptions are made of the shapes of either source distribution or attenuation media. These structures are extracted from the emission and transmission data input. We have shown [1] that the use of Monte Carlo can be very precise and valuable in estimating scatter if the modeling is done in detail. Such modeling of scatter in the context of 3-D whole body imaging is also useful for image reconstruction methods that utilize prior information of the scatter distribution.

This paper describes the 3-D PET Monte Carlo scatter correction technique extended to whole body imaging, including an improved edge detection calculation for inhomogenous media, the assumptions made and some of the results obtained for a human thorax study. The large computational burden required of a reasonably high statistics Monte Carlo calculation may necessitate the use of faster hardware or parallel computing to make this approach feasible for routine clinical use. Execution time can also be reduced by using suitable coarse sampling of the input image with little loss in accuracy [1]. The goal of this work is to demonstrate the ability of the Monte Carlo simulation to accurately model and correct for Compton scatter for complex 3-D activity distributions and attenuating media present in the human thorax.

There are three conditions that allow this approach to be feasible: (1) The scatter distribution from a patient in PET

0-7803-3180-X/96$5.00©1996

consists of relatively low spatial frequency information. A low resolution calculation with relatively few noisy data points followed by interpolation should be within the experimental accuracy of PET. (2) The 3-D nature of the simulation allows a more efficient use of simulated events. In a 2-D simulation an event that scatters out of the plane is discarded and the next event initiated. In 3-D, a large fraction of such events still interact with a detector and are counted as useful events. (3) A parallel processing workstation can be used to speed up the computation times.

## II. METHODS

The Monte Carlo scatter correction is isotope distribution dependent, and requires the 3-D reconstructed image volume of the body as input. Corrections for normalization and attenuation are assumed to be accurate. The attenuation correction was performed using a hybrid technique [2] that requires a short transmission scan from which a segmented image volume of the lungs is derived. We use this segmented image volume to determine the attenuation media boundaries. The image volume is treated as an initial estimate of the 3-D source intensity distribution for a photon tracking simulation: It is assumed that the number of counts in each pixel of the input image volume represents the true isotope concentration at that location in the body. The presence of scatter in the input images results in an overestimation of the amount of scatter calculated by the Monte Carlo. The extent of this overestimation depends on the physical situation and was measured to be $\leq 5\%$ for the brain [1] (in that paper we found that statistical fluctuations in the data are greater than the systematic negative errors introduced in the correction by including scatter in the Monte Carlo input). The effect of scatter in the simulation input data is limited because in the estimation of the scatter distribution to be subtracted in the correction, the ratio of the simulated scatter to totals distribution is used. Since these latter quantities were derived from input that included scatter, by forming this ratio the effect of the input scatter component is somewhat removed. If desired, the correction could be applied iteratively to reduce the error introduced by the presence of scatter in the input.

The image volume planes are stacked and placed in the simulated scanner, assuming a common axis. The geometry of the detector gantry is determined by the number and size of the individual detector crystals per ring (784 for the CTI 961 scanner), including spaces (0.3 mm). The program follows the history of each photon and its interactions (Compton Scatter, Photo-absorption) in the scatter medium and traces escaping photons into the detector gantry in a simulated 3-D PET acquisition. The distributions of unscattered and total (scattered + unscattered) photon pairs are calculated and sorted into their respective sinograms. The scatter component is equal to the difference between these two generated sinograms. The scatter correction is obtained by subtracting the calculated scatter distribution (see Section III-C) from the original normalized data set, when both data sets are normalized to the same number of counts.

The flow chart for the simulation was shown and described in [1]. The assumptions made in the new calculation are (a) that a photon is detected where it strikes a detector surface, provided its energy is above a certain threshold and (b) that there are two attenuating media, the lung and water. Multiple Compton scatters are allowed. The decision as to whether or not a given photon scatters in a given medium is determined by both the linear attenuation coefficient of that medium and the distance from the photon's origin in the medium to the edge of the scatter medium along the line of propagation. For human studies, the edge is determined by the segmented image used in the hybrid attenuation correction calculation [2] for the input whole-body image volume. The average value of the attenuation coefficient of the lung extracted from the attenuation file was 0.0329 $cm^{-1}$. Photon pairs originating from emission activity outside the segmented transmission image volume (and, therefore outside the body) for a given plane are not followed. This eliminates the contribution of the activity from scatter or artifacts outside the boundaries of interest. For phantoms, the edge is defined by their known geometrical shape. The energy and direction of a scattered photon is randomly determined by following the Klein-Nishina probability distribution. If the photon escapes the boundary of the body and intersects a detector in the gantry, the event is recorded in the appropriate sinogram as either a scatter or primary event depending on its energy. The energy threshold was set at 250 keV for these simulations.

The Monte Carlo 3-D whole body scatter calculation is general and can be applied to any scanner configuration or geometry. The calculation was tested using 3-D acquired images of the human thorax from the CTI 961 ECAT EXACT-HR system as input. The image volume had 89 image planes, corresponding to data acquired in two bed positions centered about the heart and lungs with a 5 plane overlap of the axial field of view. The planes were separated by 3.1 mm and composed of 128x128, 4.3 mm pixels. The Monte Carlo calculation performs a simulated 3-D PET acquisition of one bed position (24 detector rings) of the scanner axially centered over the lungs and heart. Activity outside the FOV of the simulated scanner (data from approximately 15 planes above and 27 below the FOV, which includes activity from the liver) was incorporated and 576 sinograms were created for both the unscattered and total photon pairs detected for that simulated bed position. Using a "mash" (averaging) over two angles in the simulated acquisition, this corresponds to 76 MB of data for each sinogram generated.

## III. RESULTS

### A. Axial Opening Angle Dependence of the Scatter

Figure 1 (top) displays a schematic representation in coronal cross-section of two photons being emitted (a typical "scattered" event) in the scanner in a simulated 3-D PET acquisition; the axial opening angle $\alpha$ is defined as the angle that the direction of one of the emitted photons in a pair makes with the transverse plane; in general, $\alpha$ varies from 0 to 180°. However, in the simulation, there is a maximum range of $\alpha$ above which the calculated scatter fraction does not increase, mostly due to the escape of at least one photon per annihilation pair event. The bottom portion of Figure 1 shows the manner in which the calculated scatter fraction varies with the maximum axial opening angle $\alpha$ allowed for the first photon in every photon pair event of the simulation. For an axial opening angle range near 45° the scatter fraction

(scatter/trues) in a human thorax saturates at roughly 1.2 (there are 20% more scatters than trues). In order to reduce the number of lost events, $\alpha$ was allowed to vary from 0 to a maximum value of 45° in further simulations.

## B. Accuracy of the Modeling

Figure 2 shows one plane from the input emission image (with normalization and attenuation correction) and segmented transmission image volumes representing, respectively, the isotope concentration and attenuation media boundaries to be used in the Monte Carlo. For a simulated 3-D acquisition, the data generated will in general have less counts than the input images.

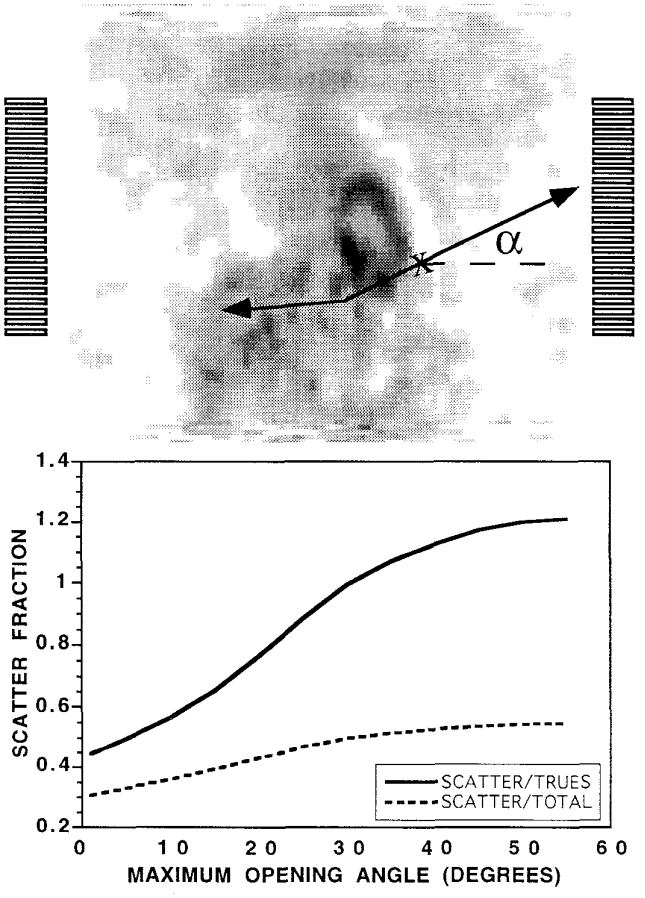


Fig. 1. Top: schematic representation of a coronal cross-section through the simulated 3-D PET scanner showing the opening angle $\alpha$ (the angle of emission transverse to the plane) of one of the photons from a pixel in the input patient image volume. A typical scatter event is shown with the photons propagating toward the detector gantry. Bottom: calculated scatter fraction vs. maximum opening angle allowed for the first photon emitted in each event in the simulation (trues = unscattered, total = trues + scattered). For $\alpha$=45°, the scatter/trues fraction saturates at a value of 1.2. Note a significant amount of activity from outside the FOV (including that from the liver) is included as input.

Figure 3 shows a comparison between a typical plane from the sinogram and input image volumes of a 3-D acquired data set (without scatter or attenuation correction) and the corresponding Monte Carlo totals data generated from a simulated 3-D PET acquisition. All image reconstructions were performed with a ramp filter at Nyquist frequency and only direct planes were reconstructed (in 2-D). In order to facilitate a comparison between the measured data and simulated output we form the *fractional difference image* when the two images (or sinograms) are normalized to the same number of counts.

The simulated sinogram and image correspond well with the measured data, indicating that the geometry and physics are adequately modeled: the rms percent deviation about zero of the fractional difference image was about 7% for both the image and sinogram data. Part of this discrepancy is explained by (1) the slight inefficiency of the image segmentation in properly locating the edges of the different density structures involved and (2) by the approximation of constant lung and soft tissue densities. Note how the boundaries of the simulated image data in Fig. 3 (bottom middle image) seem to match those of Fig. 2b rather closely. Neglecting the activity seen outside the body boundaries, which is not incorporated into the simulation, the largest difference is at the boundary of the body. Within the body boundary, the corresponding rms deviation value was roughly 5%. The fractional difference sinogram and image in Fig. 3 is consistent with the fact that inside the boundary of the body, the largest error in our normalized comparison image occurs where the activity is lower in the original image: A noise pattern is seen corresponding to the lower count structures. Likewise, the bright heart and lung areas are seen as lower count regions in the difference images.

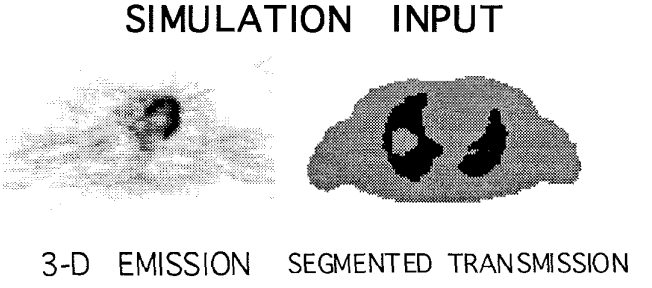


Fig. 2. Input to the Monte Carlo scatter calculation. (a) One plane from the input emission image with attenuation correction and normalization and (b) tri-level segmented transmission image. These image volumes represent, respectively, the input isotope distributions and scatter medium boundaries used in the simulation.

## C. Subtraction of the Scatter Component

Because of the lower number of events in the Monte Carlo generated data sets as compared to the input (see Fig. 3), it was necessary to scale the simulation results in order to normalize them to the measured data sets. The scale factor was derived from the ratio between the scatter plus true simulated data and the uncorrected data from the scanner. The scatter correction is obtained by subtracting the smoothed, scaled calculated scatter estimation from the original data set with normalization. After scatter subtraction, the corrected 3-D data set is smoothed, corrected for attenuation and then reconstructed using a ramp filter at the Nyquist frequency. Figure 4 displays one sinogram

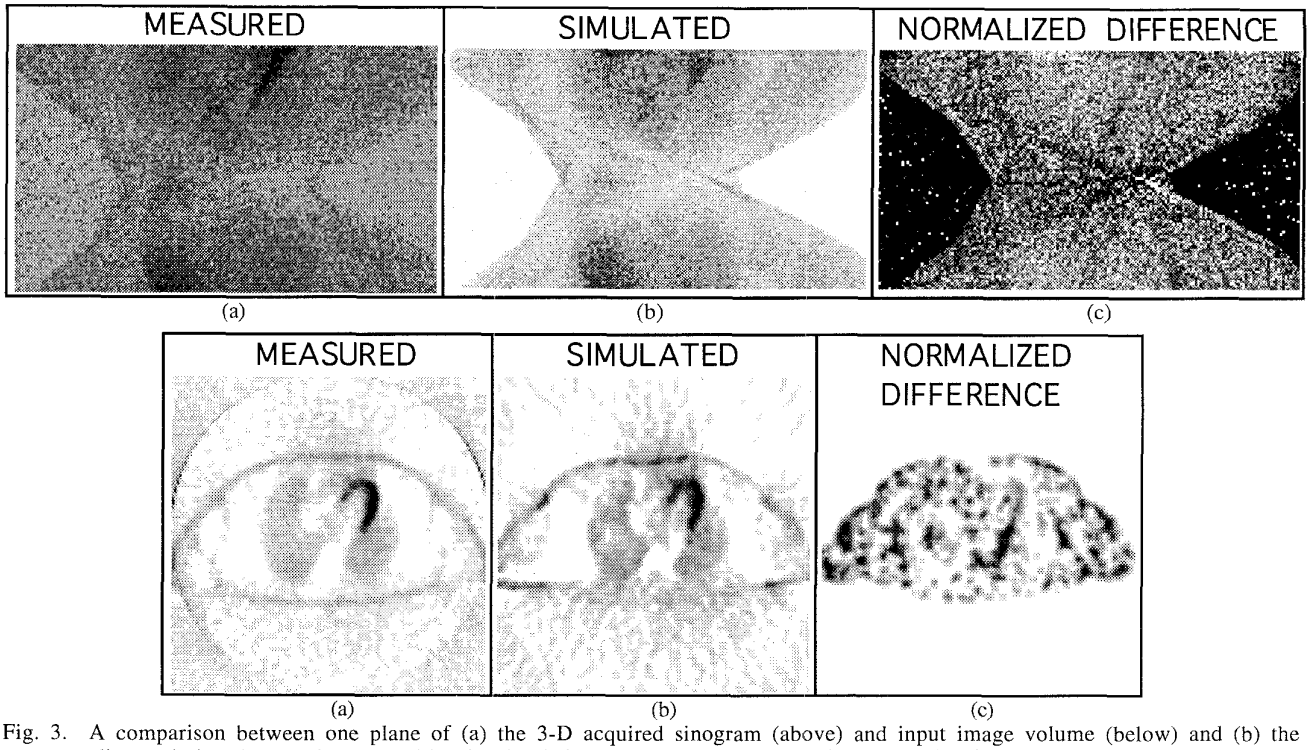


Fig. 3. A comparison between one plane of (a) the 3-D acquired sinogram (above) and input image volume (below) and (b) the corresponding emission data total generated by the simulation for a human thorax study . Note the simulated data has less events than the input image. (c) the fractional difference between (a) and (b) when the two are normalized to the same total number of counts. Only activity within the boundary of the body was included in the simulation.

and image plane (without and with attenuation correction) from the uncorrected and scatter corrected 3-D thorax study used above. The corrected images have poorer signal-to-noise ratio but better overall contrast than the uncorrected original images. Profiles through the emission data before and after the Monte Carlo calculated corrections are also shown. Since the input image volume already contained scatter, the calculation will over estimate the scatter; scatter subtraction thus resulted in some negative values. We note because of the poor noise level of the input images, it is difficult to see the effect of the scatter correction in the images shown.

### *D. The Computation Time of the Simulation*

The input image volumes discussed above were sampled pixel by pixel in the Monte Carlo simulation. Using this fine sampling the total execution time of the program was, for most cases, approximately 20 CPU hours using a Sun Sparc Station10. If we assume that the Compton scatter distribution is slowly varying over the object, coarser sampling of the input image volume is justified. By sampling over regions equivalent to 4x4 pixels, the execution time of the calculation was reduced by over an order of magnitude to just over an hour. Figure 4 shows smoothed profiles through simulated total, primary and scatter sinograms. The scatter calculation profile is shown for both fine and coarsely sampled input. The two calculated scatter distributions compare well (overall to within 6% in mean number of counts) indicating that little error in the calculation of the scatter contribution is introduced by coarser sampling. For the finely-sampled simulation, scattered events comprise approximately 120% of the primary photon pairs detected.

Since one of the goals in this work is to preserve the accuracy of the scatter calculation, the finest sampling consistent with acceptable execution times will be used in practice. The coarser the sampling of the input image data, the worse the blurring will be in the simulated emission data sets of scattered and unscattered photons, and the less accurate the scatter estimation. It should be noted that the current software is research grade code that requires optimization. We have assembled a workstation configured as eight i860 array processors that we expect will improve the computation time by over a factor of 20 relative to a single Sparc10 CPU. Preliminary tests show that a single i860 chip was over 3 times faster than a Sparc10 CPU for calculations similar to those involved in the Monte Carlo code. With eight of such processors running in parallel, and partially vectorized code, the expected computation time of the simulation would be reduced to < 1 hour for the fine sampling case and < 3 minutes for coarse sampled input.

## IV. DISCUSSION

Our results indicate that the Monte Carlo approach to 3-D PET whole body scatter correction is highly accurate with execution times that are close to being in an acceptable range for clinical use (with coarse sampling of the input). In general, the technique requires no assumptions of the shapes of the source or scatter distributions or the physics of Compton scattering. No computational approximating techniques have yet been utilized. The scatter component of the total activity was calculated for complex activity distributions. Except for the boundaries of the body, the accuracy of the modeling is estimated to be better than 5%.

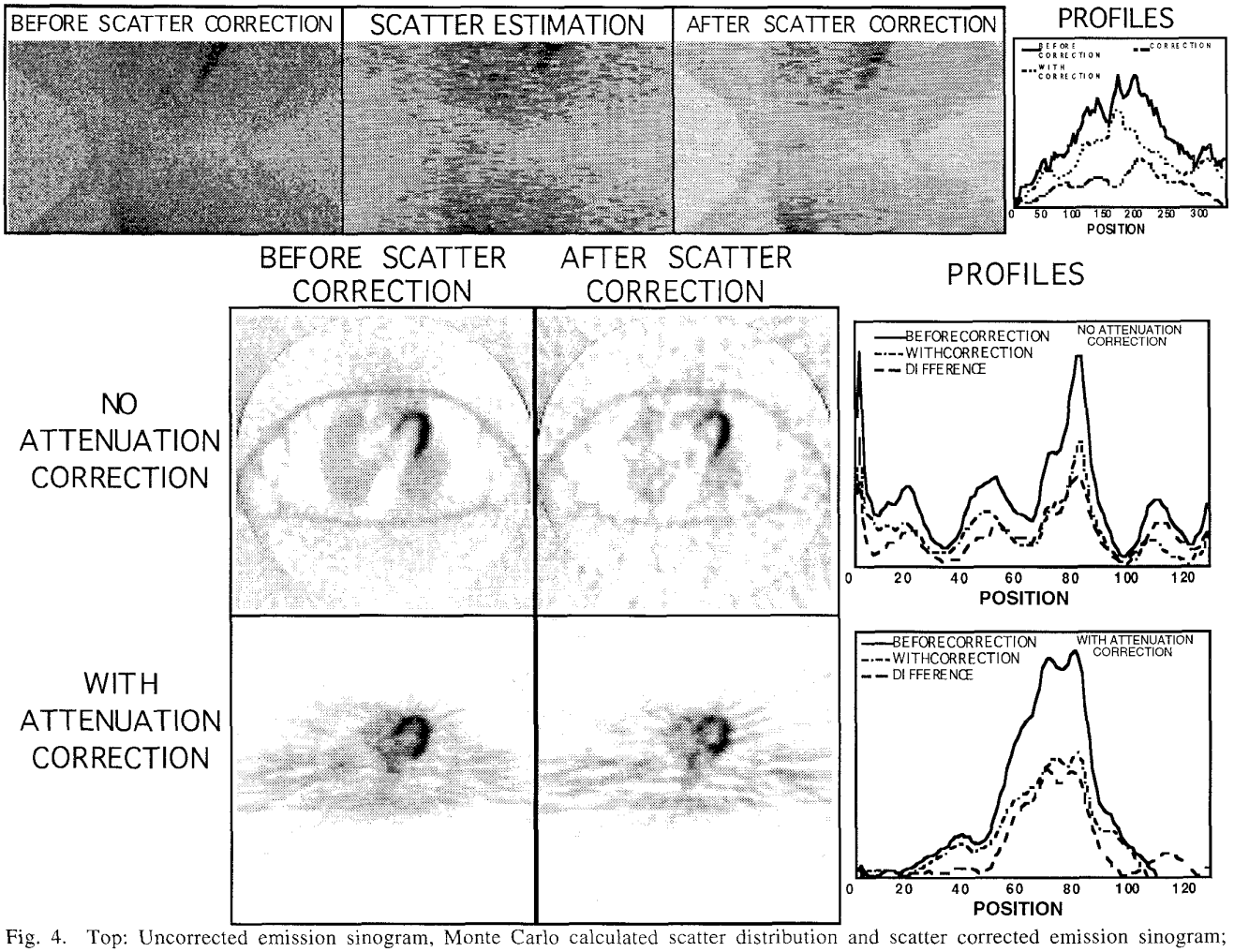


Fig. 4. Top: Uncorrected emission sinogram, Monte Carlo calculated scatter distribution and scatter corrected emission sinogram; Bottom: Corresponding reconstructed image plane with and without attenuation. Profiles through row 50 (angle 50 in sinogram and row 50 of images) are shown. There were no significant negative values.

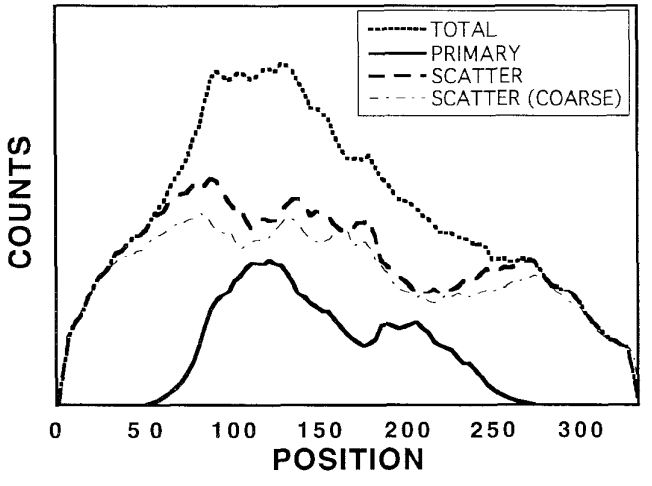


Fig. 4. Profiles through the sinograms of the Monte Carlo calculated uncorrected, corrected and scatter distributions (fine and coarse input) for a 3-D human thorax study (Legend shown at top); there were no significant negative values. The calculated scatter distributions for the coarse and finely sampled cases compare well.

Computation time for coarse sampling is nearly a factor of 16 times shorter than for fine sampling.

Images containing scatter are used as an initial estimate of the isotope distribution. This assumption results in an overestimation of the scatter. In general, the extent of the overestimation depends on the physical situation. In our previous work [1] we found that the statistical fluctuations in the activity are greater than the systematic negative errors introduced by including scatter in the input. If desired, the correction could be applied iteratively to reduce the error introduced by the presence of scatter in the simulation input. In regards to quantitation, the assumption of perfect detectors is reasonable. Small crystal size effects will not produce the large quantitative errors that scatter in the body produces.

## V. REFERENCES

[1] CS Levin, M Dahlbom, EJ Hoffman, 1995. A Monte Carlo Correction for the Effect of Compton Scattering in 3-D PET Brain Imaging. *IEEE Trans. Nucl. Sci.* In Press.

[2] YC Tai, KP Lin, M Dahlbom, SC Huang, EJ Hoffman. A Hybrid Attenuation Correction Technique to Compensate for Lung Density in 3-D Total Body PET. *IEEE Med Im Conf,* **4**:1643-7.